



Cite this: *RSC Adv.*, 2018, **8**, 2260

## Self-supporting S@GO–FWCNTs composite films as positive electrodes for high-performance lithium–sulfur batteries†

Lifeng Cui,\*<sup>a</sup> Yanan Xue,<sup>a</sup> Suguru Noda <sup>c</sup> and Zhongming Chen <sup>\*b</sup>

Although lithium–sulfur (Li–S) batteries are a promising secondary power source, it still faces many technical challenges, such as rapid capacity decay and low sulfur utilization. The loading of sulfur and the weight percentage of sulfur in the cathode usually have a significant influence on the energy density. Herein, we report an easy synthesis of a self-supporting sulfur@graphene oxide-few-wall carbon nanotube (S@GO–FWCNT) composite cathode film, wherein an aluminum foil current collector is replaced by FWCNTs and sulfur particles are uniformly wrapped by graphene oxide along with FWCNTs. The 10 wt% FWCNT matrix through ultrasonication not only provided self-supporting properties without the aid of metallic foil, but also increased the electrical conductivity. The resulting S@GO–FWCNT composite electrode showed high rate performance and cycle stability up to  $\sim 385.7 \text{ mA h g}_{\text{electrode}}^{-1}$  after 500 cycles and close to  $\sim 0.04\%$  specific capacity degradation per cycle, which was better than a S@GO composite electrode ( $353.1 \text{ mA h g}_{\text{electrode}}^{-1}$ ). This S@GO–FWCNT composite self-supporting film is a promising cathode material for high energy density rechargeable Li–S batteries.

Received 22nd September 2017

Accepted 20th December 2017

DOI: 10.1039/c7ra10498g

rsc.li/rsc-advances

## 1. Introduction

The global energy shortage and environmental pollution have accelerated the emergence of new clean power sources. On account of high volumetric and gravimetric energy density, lithium ion batteries have become the dominant power source for portable electronic devices such as laptops, watches, *etc.*<sup>1,2</sup> However, the lower specific capacity of cathode materials ( $\sim 150 \text{ mA h g}^{-1}$  for layered oxides and  $\sim 170 \text{ mA h g}^{-1}$  for LiFePO<sub>4</sub>)<sup>3,4</sup> is insufficient for the demands of electric vehicles with high energy density and power density. Therefore, it is necessary to enhance the power and energy density of present lithium ion battery systems and employ high capacity cathode materials for rechargeable lithium battery technology. Sulfur has been considered as one of the most promising cathode materials as its theoretical specific capacity of is as high as  $1672 \text{ mA h g}^{-1}$  and the theoretical energy density of Li–S battery is  $2600 \text{ W h kg}^{-1}$ .<sup>5,6</sup> In addition, elemental sulfur is non-toxic, abundant in nature, low-cost and eco-friendly. In terms of

these attractive features, the development of practical Li–S battery has been hindered by several problems associated with poor electrical conductivity of sulfur, low sulfur utilization, large volumetric expansion (80%) of sulfur upon lithiation and “shuttle effect” due to polysulfide dissolution in the electrolyte and gradual loss of active sulfur.<sup>7,8</sup>

In recent years, the compounds of various carbon materials mixed with elemental sulfur has been tested as cathode material for lithium–sulfur battery, in order to improve the electrochemical performance of sulfur cathode.<sup>9,10</sup> Among these materials, graphene is an ideal carbon matrix with its high surface area, chemical stability, mechanical strength and flexible 2D structure for lithium–sulfur battery.<sup>11</sup> Cathode materials that contain the structure of graphene wrapping on sulfur particles *via* various surfactant, have been reported previously.<sup>12,13</sup> However, polymeric binder and a metal aluminum foil used in the conventional electrode architecture decrease the fraction of the active material in the battery cells and produce the contact resistance between the active material and metal collector.

Carbon nanotubes (CNTs) possessing high tensile strength, flexibility, electrical conductivity and high SSA have become the ideal substitute for metal collector. FWCNTs (few-wall CNTs) are sub-millimeter-long, continuous and mass produced by fluidized-bed chemical vapor deposition (FB-CVD), which has advantages on the basis of cost with ease to control over SWCNTs (single-wall CNTs) and MWCNTs (multi-wall CNTs).<sup>14</sup> Furthermore, it has high mechanical strength and conductivity as high as  $100 \text{ S cm}^{-1}$  owing to the long length ( $\sim 400 \text{ mm}$ ) and

<sup>a</sup>School of Materials Science and Engineering, University of Shanghai for Science and Technology, Shanghai, 200093, China. E-mail: lcui@usst.edu.cn

<sup>b</sup>School of Environment and Civil Engineering, Guangdong Engineering and Technology Research Center for Advanced Nanomaterials, Dongguan University of Technology, Guangdong 523808, PR China. E-mail: zmchen@dgu.edu.cn; Tel: +86 76922861232

<sup>c</sup>Department of Applied Chemistry, School of Advanced Science and Engineering, Waseda University, 3-4-1 Okubo, Shinjuku-ku, Tokyo 169-8555, Japan

† Electronic supplementary information (ESI) available. See DOI: 10.1039/c7ra10498g

high aspect ratio ( $\sim 50\,000$ ).<sup>15</sup> Therefore, FWCNTs with excellent flexibility and electrical conductivity can be made into self-supporting films and applied to lithium-ion battery<sup>15,16</sup> and super-capacitor as current collector.<sup>17,18</sup> Recently, Chen *et al.* has made great progress in the flexible electrode material of Li-S battery.<sup>19</sup> They demonstrate that the flexible CNTs-RGO/S cathode exhibited discharge capacities of  $\sim 409$  and  $\sim 325\text{ mA h g}_{\text{electrode}}^{-1}$  at 0.2C and 1C, respectively, after 100 cycles. They used MWCNTs at a high content of 20 wt%, and hence, developing flexible sulfur cathode with high cycle stability and loading density is critical.

In this work, we exploit sub-millimeter-long FWCNT matrix as current collector and presents a rational design and synthesis of a self-supporting S@GO-FWCNTs composite cathode film for Li-S battery. Sulfur micro-particles, modified by sodium dodecyl benzene sulfonate (SDBS) surfactant, was uniformly wrapped by GOs with negative charges through a simple solution process, and then suspensions of S@GO and FWCNTs were mixed and filtered to get a self-supporting composite S@GO-FWCNTs film. In this well-designed structure, the GO-FWCNTs matrix buffers the volume change for sulfur particles and FWCNTs provide a fast electron pathway during charging and discharging process. Furthermore, the addition of FWCNTs not only enhance the electron transfer inside cathode materials, but also replace the metal foil current collector and increase the weight proportion of active material in cathode materials.<sup>20,21</sup> With the specific capacity of  $387.5\text{ mA h g}_{\text{electrode}}^{-1}$  after 500 cycle at the current density of 3C (1C =  $1672\text{ mA g}_{\text{sulfur}}^{-1}$ ), which is higher than that of the traditional cathodes for lithium ion battery.<sup>22,23</sup> And the comparative result with other recent report shown in Table S1 (ESI†), the S@GO-FWCNTs composite cathode showed excellent cycling stability during charge-discharge process for lithium-sulfur battery.

## 2. Experiments

### 2.1 The preparation of sulfur particles

Sulfur particles with  $\sim 500\text{ nm}$  diameter were synthesized as follows. Concentrated HCl (1.7 mL,  $11.9\text{ mol L}^{-1}$ ) was added to an aqueous solution of  $\text{Na}_2\text{S}_2\text{O}_3 \cdot 5\text{H}_2\text{O}$  (80 mL,  $0.01\text{ mol L}^{-1}$ ) with the presence of SDBS (0.5 wt%), firstly. After reaction of  $\text{Na}_2\text{S}_2\text{O}_3$  and HCl for 2 hours, the product was washed by deionized water for three times, and dried at  $60\text{ }^\circ\text{C}$  for 12 h under vacuum. Then sulfur particles were obtained.

### 2.2 The synthesis of S@GO composite

S particles and GO were firstly dispersed in HCl (1 M) solutions separately. After sonicating for 30 minutes with the temperature of less than  $20\text{ }^\circ\text{C}$ , the two suspensions were mixed and stirred for 2 hours. After keeping for 8 hours, the precipitate was washed by deionized water and EtOH successively using centrifuge. Finally S@GO was dispersed in EtOH. The S@GO composites were prepared with different weight ratios of 1 : 1, 3 : 1, 5 : 1.

### 2.3 S@GO-FWCNTs composite synthesis

Sub-millimeter-long FWCNTs produced by FBCVD reactor with the characteristic of 6–10 nm diameter, 0.4 mm length, 99.6–99.8 wt% purity,  $400\text{ m}^2\text{ g}^{-1}$  SSA, triple-walls on average.<sup>14</sup> FWCNTs were dispersed in EtOH by ultrasonication at a concentration of  $0.1\text{ mg mL}^{-1}$  with the temperature less than  $20\text{ }^\circ\text{C}$  for 30 minutes. In order to keep the structure of the S@GO, the dispersed FWCNTs/EtOH solution was mixed with S@GO/EtOH solution (the weight ratio of 3 : 1) by magnetic stirring. After 30 min, the system was vacuum-filtrated by a membrane filter with the filter membrane of polytetrafluoroethylene (0.45  $\mu\text{m}$  pore size), and the product film was separated from the membrane using tweezers. Next, the film was dried at  $80\text{ }^\circ\text{C}$  for 12 hours in air followed by vacuum drying at  $60\text{ }^\circ\text{C}$  for 12 hours. The density and thickness of the best S@GO-FWCNTs film (S : GO = 3 : 1 with 10 wt% FWCNTs) were  $\sim 0.22\text{ mg cm}^{-2}$  and  $\sim 1.2\text{ }\mu\text{m}$ , respectively.

### 2.4 Electrochemical measurement

S@GO-FWCNTs samples were made into self-supporting films and cut into small round disks and directly used as the working electrode in coin type lithium ion cells. S@GO samples were in powder form and could not form continuous self-supporting films. Super P (carbon black) conductive filler and PVDF (polyvinylidene fluoride) binder were mixed with S@GO powders by weight of 1 : 1 : 8 in NMP (*N*-Methyl Pyrrolidone) to form slurry. Then, the slurry was coated on aluminum foil using a doctor blade and dried at  $80\text{ }^\circ\text{C}$  for 12 hours in air first and  $60\text{ }^\circ\text{C}$  for 12 hours in vacuum to form the working electrodes. 2032-type coin cell was assembled in an argon-filled glovebox ( $\text{O}_2$  and  $\text{H}_2\text{O}$  level both below 0.1 ppm) and contained a lithium metal counter electrode, Celgard 2500 separators, and electrolyte of 1 M LiTFSI (lithium bis(trifluoromethane sulfonyl)imide) in 1 : 1 v/v DME (1,2-dimethoxyethane) and DOL (1,3-dioxolane) containing 1 wt% LiNO<sub>3</sub>. The 2032-type coin cell was tested electrochemically using a LAND CT2001A instrument under room temperature in the voltage range 1.7–2.6 V. The cyclic voltammetry (CV) data were collected with CHI760E at a scan rate of  $0.1\text{ mV s}^{-1}$  between 1.7 and 2.6 V.

## 3. Result and discussion

### 3.1 The S@GO cathode materials

The schematic diagram of the S@GO-FWCNTs composite was shown in Fig. 1a, and the detail description was shown in Experiments. From Fig. 1b, we observed the pristine FWCNTs express graininess-like after shaking. And the dispersed FWCNTs by ultrasonication for 30 min had a stable dispersion and no precipitation after 30 min as shown in Fig. 1c. In addition, Fig. 1d reveals the produced composite film to be flexible.

The scanning electron microscopy (SEM) (JMS-6701F, Japan) analysis displayed the morphological characteristics of the as-synthesized materials. SEM images of sulfur particles by *in situ* synthetic ways were shown in Fig. 2a. In our approach, sulfur particles were made through the *in situ* reaction of sodium thiosulfate pentahydrate ( $\text{Na}_2\text{S}_2\text{O}_3 \cdot 5\text{H}_2\text{O}$ ) with HCl in



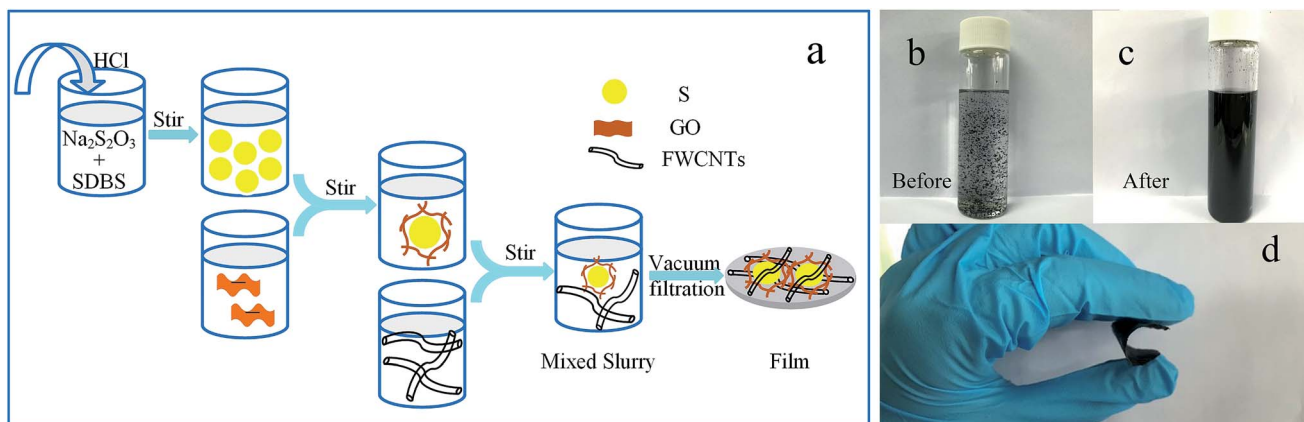


Fig. 1 (a) Schematic diagram of the fabrication of S@GO–FWCNTs composite. (b) Optical image of FWCNTs solutions before sonication and after shaking. (c) Optical image of FWCNTs solutions after sonication for 30 min and keeping for 30 min. (d) Optical image of the S@GO–FWCNTs composite film.

an aqueous solution. We can clearly see that the sulfur particles, synthesizing along with SDBS (Fig. 2a), had more inerratic shapes and homogeneous distributions. Besides, the diameter of sulfur is shown in the insert histograms, showing that most of the particles had a size around 500 nm. It illustrates that the size-engineering of the sulfur particles could attribute to the synergistic effect of SDBS by controlling the nucleation and growth process. Fig. 2d shows the SEM of the as-prepared S@GO composite materials (the S : GO weight ratio of 3 : 1) revealing GO sheets well coating sulfur particles. This special structure may be contributed to a way for GO to minimize the surface energy in the ionic solution. When GO coated the sulfur particles, it would lose the inner side of its surface and form a core–shell structure.<sup>24</sup> A higher magnification SEM image

(Fig. 2e) of Fig. 2d obviously showed the structure of S particles which wrapped up in the GO. In order to obtain the best performance of the Li–S battery, we examined different weight ratios of sulfur to GO in this experiment. From Fig. 2b, we can obviously observe that GO coated on sulfur massively with the S : GO weight ratio of 1 : 1. Fig. 2c revealed the S@GO at the weight ratio of 5 : 1 contained excessive sulfur particles in the mixture. The characteristic of the S@GO–FWCNTs composite materials are shown in Fig. 2f. From Fig. 2f, FWCNTs evenly dispersed in the as-prepared S@GO hybrid materials. The higher magnification SEM image in Fig. 2f revealed FWCNTs, which were intertwined with one another, showing a web structure, and indicated the sulfur was embedded in the FWCNTs web structure to form an inseparable complex. The

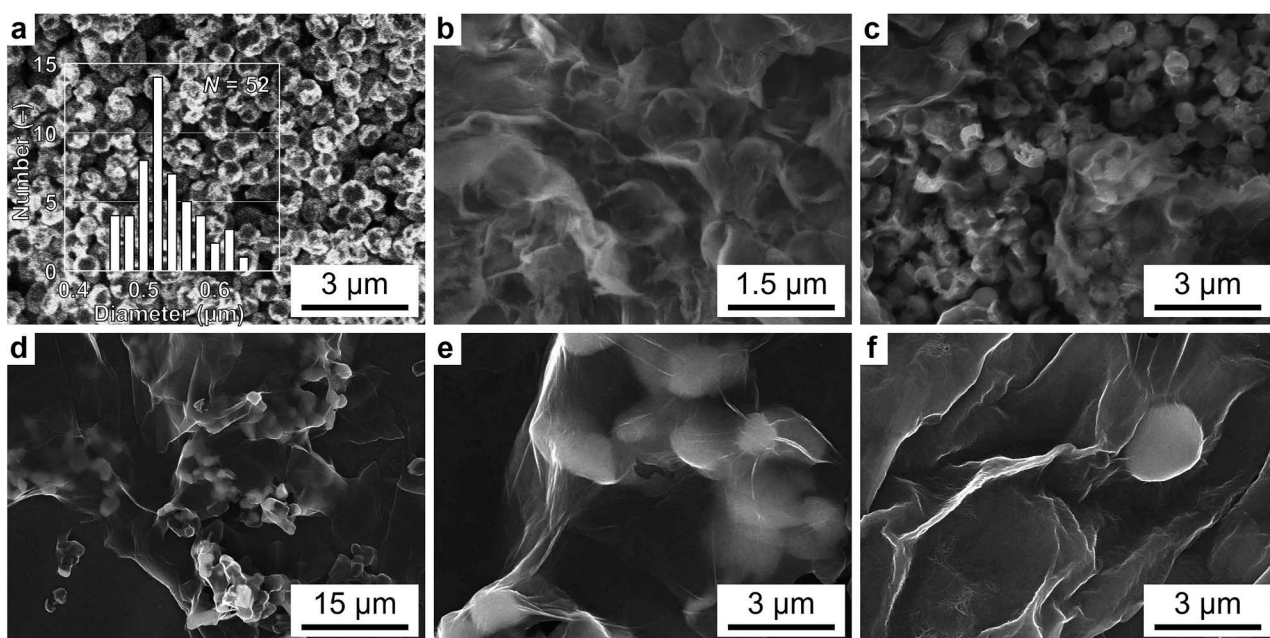


Fig. 2 SEM images of S (a), S@GO (the weight ratio of sulfur to GO in 1 : 1 and 5 : 1) (b and c), S@GO (the weight ratio of sulfur to GO in 3 : 1, at low and high magnifications) (d and e), and S@GO–FWCNTs (the weight ratio of sulfur to GO in 3 : 1 and the mass fraction of FWCNTs of  $\approx 10\%$ ) (f).

FWCNT matrix held the S@GO particles well by the strong van der Waals interaction owing to the small diameter and large specific surface area of the long FWCNTs.

The XRD analysis relating to the detailed structure of pure S, GO and S@GO hybrid was shown in Fig. 3a. The pure sulfur presented very sharp and strong peaks in the whole diffraction range, which correspond to a well-defined crystal  $S_8$  structure. Graphene oxide showed a typical XRD pattern with three peaks at  $11^\circ$ ,  $25^\circ$  and  $43^\circ$ . After the formation of S@GO composite, all the other diffraction peaks accord with the  $S_8$  structure, indicating that sulfur in S@GO composite is crystalline without formation of carbon–sulfur compounds during the process of synthesis.

Fig. 3b, the thermos-gravimetric analysis (TGA), determined that the sulfur loading is 72.1 wt% in S@GO composite (3 : 1) and the S@GO–FWCNTs composites have 66.1 wt% sulfur content. The thermos-gravimetric curves of different S : GO weight ratios in Fig. 3b showed that the sulfur content were 47.9 and 75.9 wt% (S : GO = 1 : 1 and S : GO = 5 : 1), respectively.

To further analyze the electrical performance of S@GO of different weight ratios, we conducted the galvanostatic charge/discharge measurements. As shown in Fig. 4, the initial capacities of 370, 470 and 454.3 mA h  $g_{\text{electrode}}^{-1}$  were respectively achieved for the S : GO weight ratios of 1 : 1, 3 : 1 and 5 : 1. The S@GO cathode with the 1 : 1 ratio showed the smallest specific capacity due to the smallest S content. And after 500 cycles, the S@GO cathode, relating to the various weight ratio of sulfur to GO, decline just almost 0.05% specific capacity degradation per cycle. It is an evidence that sulfur was wrapped by GO well and the structure of S@GO is stable. Furthermore, the cathode with the S : GO weight ratio of 3 : 1 had 353.1 mA h  $g_{\text{electrode}}^{-1}$  after 500 cycle at 3C (1C = 1672 mA  $g_{\text{sulfur}}^{-1}$ ). And it was better than the cathode with the 5 : 1 ratio. The possible reason was that the excessive sulfur in the S@GO cathode with the 5 : 1 ratio was not covered by GO, which makes polysulfide dissolve into the electrolyte, transform to  $\text{Li}_2\text{S}/\text{Li}_2\text{S}_2$  in the first place. The

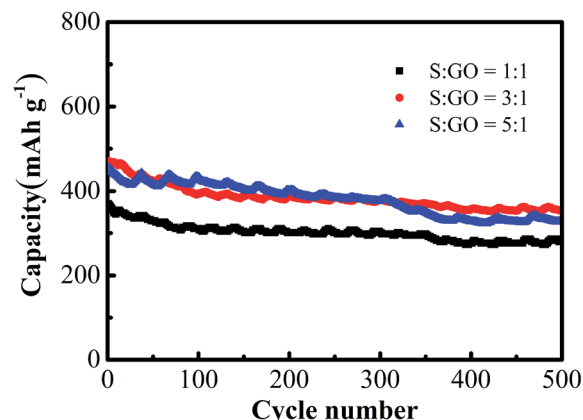


Fig. 4 Cycling performance of S@GO with different weight ratios at 3C (1C = 1672 mA  $g_{\text{sulfur}}^{-1}$ ).

resulting  $\text{Li}_2\text{S}/\text{Li}_2\text{S}_2$  would encapsulate and hinder sulfur contributing to the charge–discharge process.

Although the conventional Li–S battery preferred to use aluminum foil for charge collection, the utilization of sulfur in the cathode materials was lower. Owing to the high conductivity, FWCNTs matrix can be regarded as current collector. The following electrochemical test were aimed to research the performance of the film cathode, containing FWCNTs matrix, and compare it with metal collector cathode.

### 3.2 The S@GO–FWCNTs cathode materials

A comparative XPS study was done in order to understand the chemical composition and surface properties of S@GO–FWCNTs composite and the result was shown in Fig. 5. In the S 2p spectrum of the S@GO–FWCNTs composite (Fig. 5a), the S 2p<sub>3/2</sub> (164.0 and 165.2 eV) corresponded to the S–S bond, and another small peak located at 168.8 eV was identified as the sulfate species deriving from a trace residue of sulfate.<sup>10</sup> The above analysis demonstrated that the sulfur mostly retained the

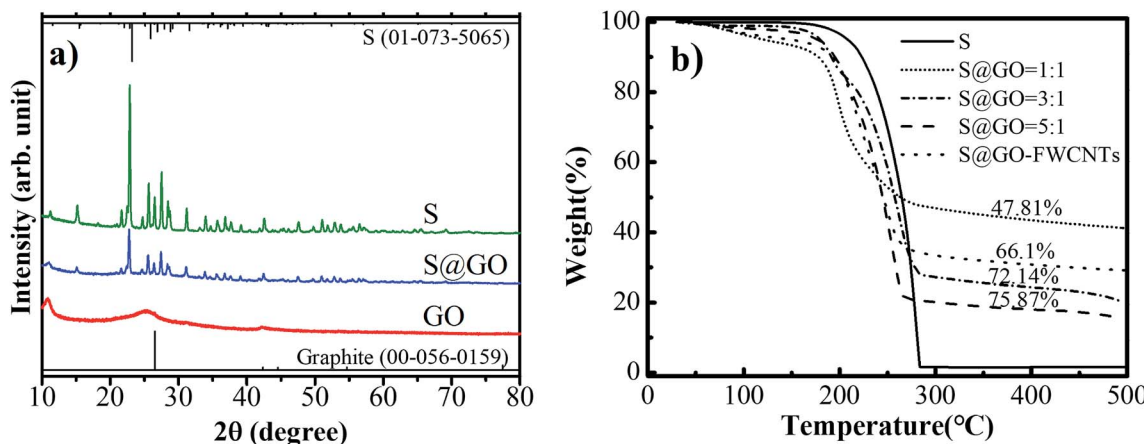


Fig. 3 (a) XRD patterns of S, GO, and S@GO hybrid; (b) thermogravimetric (TG) curves of S, S@GO, and S@GO–FWCNTs (for S@GO, the weight ratios of S to GO are 1 : 1, 3 : 1 and 5 : 1, respectively, and for S@GO–FWCNTs the weight ratio of S to GO is 3 : 1 and the overall weight percentage of FWCNTs of  $\approx 10$  wt%).



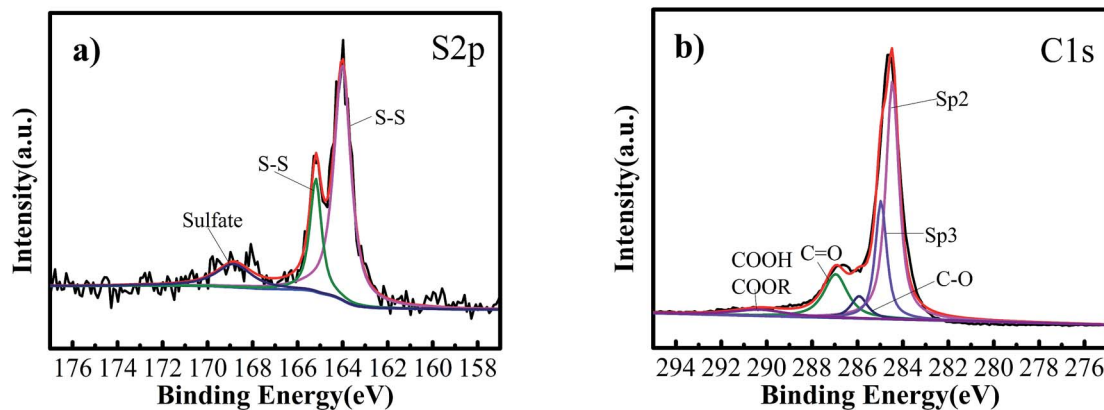


Fig. 5 (a) S 2p X-ray photoelectron spectroscopy (XPS) spectra of S@GO-FWCNTs composite. (b) C 1s XPS spectra of S@GO-FWCNTs composite.

bulk state, in consistence with the XRD results. As Fig. 5b shows, apart from the peaks centered at 284.5 and 285.0 eV corresponding to C=C and C-C in pristine FWCNTs, respectively,<sup>25,26</sup> there were three different peaks centered at 286.0, 286.9 and 290.3 eV, corresponding to the C-O, C=O and O=C-O functional groups, respectively. These oxygen-containing groups may be attributed to GO in the composite.<sup>10,27,28</sup> After the formation of S@GO-FWCNTs, a sharp peak of the C=C bond is confirmed in the peak fitting result. It revealed that the S@GO embedded in the FWCNTs web structure. S was encapsulated by GO, which can limit polysulfide dissolution.<sup>24</sup> Furthermore, the sheet conductivity of the self-supporting S@GO-FWCNTs films, evaluated through a four-probe method, was 5 S cm<sup>-1</sup>, which showed good conductivity of the cathode material and benefited the charge transfer despite of the small FWCNT content of 10 wt%.<sup>29</sup> Note that the pure FWCNT film has even higher conductivity (100 S cm<sup>-1</sup>) because of the long length (~400 mm) and high aspect ratio (~50 000) of the FWCNTs.<sup>15</sup>

Fig. 6a revealed discharge-charge profiles of the S@GO and S@GO-FWCNTs cathode between 1.7 and 2.6 V at the current density of 0.2C. Both of the two cathodes express two distinct reduction voltage plateaus and one oxidation voltage plateau. During the reduction process of S@GO-FWCNTs, two pronounced reduction peaks around 1.98–2.06 V and 2.25–2.34 V were observed. The peak at 2.25–2.34 V was

a representation of the transformation of sulfur to higher-order polysulfide ( $\text{Li}_2\text{S}_x$ ,  $4 < x < 8$ ),<sup>30</sup> while the peak at 1.98–2.06 V corresponded to the reduction of higher-order polysulfide to lower-order polysulfide ( $\text{Li}_2\text{S}_x$ ,  $2 \leq x \leq 4$ ).<sup>31</sup> In the following oxidation process, only one sharp oxidation peak at the potential of 2.3–2.42 V was observed and can be attributed to the conversion of lithium sulfides to sulfur.<sup>12</sup> Compared with the charge-discharge curve of S@GO, the curve of S@GO-FWCNTs revealed that the reduction peaks was slightly higher and the oxidation peaks is lower. It is likely due to the FWCNTs web structure, which could benefit the charge transfer owing to the high conductivity of FWCNTs matrix.<sup>14,29</sup> On the other hand, the flexible composite film with 3D FWCNTs networks can buffer the volume change during cycling and avoids destruction of the electrode.<sup>29</sup>

To further verify the electrochemical performance of S@GO cathode and S@GO-FWCNTs cathode, the cells were cycled at varied current rates (as shown in Fig. 6b). When the cells were operated at 0.1C, 0.2C, 0.5C, 1C, 3C and 5C, the S@GO-FWCNTs electrode exhibited a stable capacity of 1005.1, 843.7, 765.5, 599.3, 496.3 and 359.7 mA h g<sup>-1</sup> electrode<sup>-1</sup>, respectively. And when the rate was returned to 1C and 0.2C after high current density testing, the specific capacity of the S@GO-FWCNTs cathode electrode reverted to 565 and 643.3 mA h g<sup>-1</sup> electrode<sup>-1</sup>, implying stability capacity and reversibility.

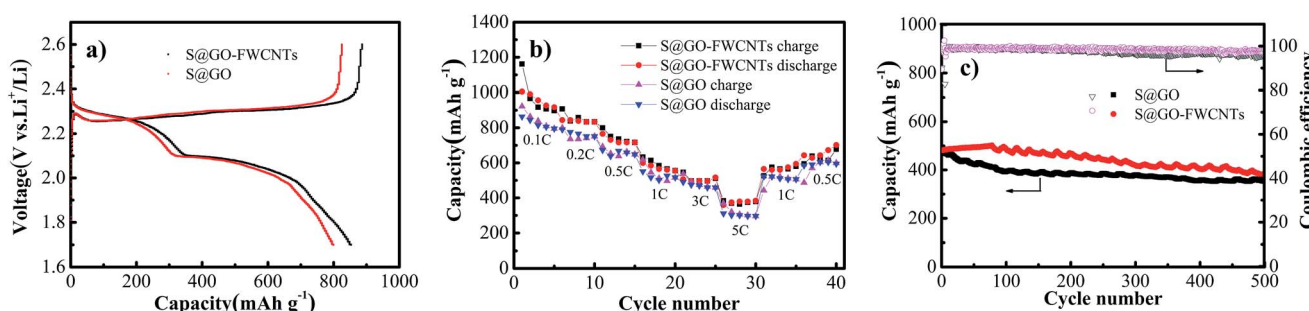


Fig. 6 (a) Discharge-charge profiles of S@GO and S@GO-FWCNTs at 0.2C. (b) Rate capability of S@GO and S@GO-FWCNTs. (c) Cycling performance and coulombic efficiency of S@GO and S@GO-FWCNTs at 3C for 500 cycles (1C = 1672 mA g<sup>-1</sup> sulfur<sup>-1</sup>).

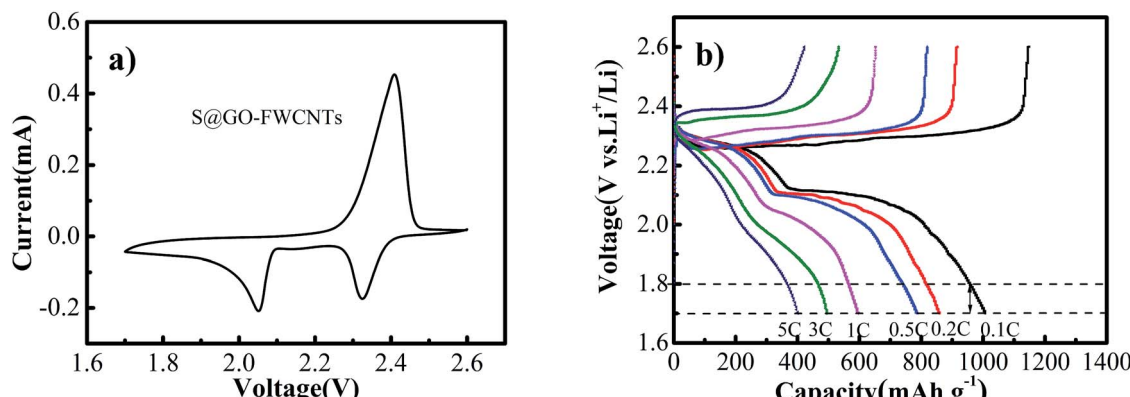


Fig. 7 (a) Cyclic voltammetry curve of S@GO-FWCNTs at  $0.1 \text{ mV s}^{-1}$ ; (b) discharge-charge profiles of S@GO-FWCNTs at different current rates.

In order to evaluate the Li-S battery performance, we carried out galvanostatic charge/discharge tests within voltage range of 1.7–2.6 V at a current density of 3C (Fig. 6c). As shown in Fig. 6c, we observed initial discharge capacities of 470 and  $482.1 \text{ mA h g}_{\text{electrode}}^{-1}$  for the S@GO and S@GO-FWCNTs cathodes, respectively. And then after 500 cycles, the S@GO-FWCNTs cathode exhibited  $385.7 \text{ mA h g}_{\text{electrode}}^{-1}$  with a specific capacity degradation per cycle of  $\sim 0.04\%$ . In addition, the coulombic efficiency was 90.3% in the first cycle and higher than 98% on average. According to the Table S1 (ESI†), the conductive film of this work showed high cycle stability.

Fig. 7a revealed the cyclic voltammetry curves of S@GO-FWCNTs cathode between 1.7 and 2.6 V at a scan rate of  $0.1 \text{ mV s}^{-1}$ . And the figure of cathodes expressed two distinct reduction peaks (at 2.05 and 2.32 V) and one oxidation peak (at 2.4 V). It further proved the typical peaks of the electrode in the CV curves correspond well to the positions of the plateaus (Fig. 6a). Fig. 7b showed galvanostatic charge and discharge voltage profiles of S@GO-FWCNTs at various current densities within the voltage range of 1.7–2.6 V. These result were consistent with the CV result in Fig. 6b, and the decreasing capacity at increasing rate is accompanied with the increasing overvoltage. The FWCNTs matrix can add the self-supporting nature and electric conductivity to the S@GO but cannot enhance the ion diffusion in the electrolyte and charge transfer between the electrolyte and S@GO. Some other measure is needed to improve the high-rate performance further.

## 4. Conclusions

We successfully synthesized the binder-free and self-supporting S@GO-FWCNTs compound film electrode *via* vacuum filtration as cathode in Li-S battery. The FWCNT matrix, improving the conductivity of the active material and increasing the weight percentage of sulfur, is an ideal current collector. The free-standing and flexible composite S@GO-FWCNTs films, showing significant improvements over S@GO composite material in specific capacity and energy density, are promising cathode materials for high energy density rechargeable Li-S batteries. More investigation is underway to further enhance

the cycling performance of this composite film, such as changing the amount of added FWCNTs and improving the dispersion of FWCNTs.

## Conflicts of interest

There are no conflicts to declare.

## Acknowledgements

We thank the financial support of the National Natural Science Foundation of China (Grant No. 51671136, 51528202 and 21706030), Guangdong Youth Innovation Project for Colleges and Universities (Grant No. 2015KQNCX164). SN thanks JSPS for support through Kakenhi grant JP16H06368.

## References

- 1 M. Armand and J. M. Tarascon, Building better batteries, *Nature*, 2008, **451**, 652.
- 2 B. L. Ellis, K. T. Lee and L. F. Nazar, Positive Electrode Materials for Li-Ion and Li-Batteries, *Chem. Mater.*, 2009, **22**, 691.
- 3 C. D. Liang, N. J. Dudney and J. Y. Howe, Hierarchically Structured Sulfur/Carbon Nanocomposite Material for High-Energy Lithium Battery, *Chem. Mater.*, 2009, **21**, 4724.
- 4 G. Y. Zheng, Y. Yang, J. J. Cha, S. S. Hong and Y. Cui, Hollow Carbon Nanofiber-Encapsulated Sulfur Cathodes for High Specific Capacity Rechargeable Lithium Batteries, *Nano Lett.*, 2011, **11**, 4462.
- 5 J. B. Goodenough, Electrochemical energy storage in a sustainable modern society, *Energy Environ. Sci.*, 2013, **7**, 14.
- 6 N. R. Van, Sulphur back in vogue for batteries, *Nature*, 2013, **498**, 416.
- 7 S. Chen, X. Huang, B. Sun, J. Zhang, H. Liu and G. Wang, Multi-shelled hollow carbon nanospheres for lithium-sulfur batteries with superior performances, *J. Mater. Chem. A*, 2014, **2**, 16199.



8 Y. Yang, G. Zheng and Y. Cui, Nanostructured sulfur cathodes, *Chem. Soc. Rev.*, 2013, **42**, 3018.

9 W. Z. Bao, D. W. Su, W. X. Zhang, X. Guo and G. X. Wang, 3D Metal Carbide@Mesoporous Carbon Hybrid Architecture as a New Polysulfide Reservoir for Lithium–Sulfur Batteries, *Adv. Funct. Mater.*, 2016, **26**, 8746.

10 S. Z. Niu, W. Lv, C. Zhang, Y. T. Shi, J. F. Zhao, B. H. Li, Q. H. Yang and F. Y. Kang, One-pot self-assembly of graphene/carbon nanotube/sulfur hybrid with three dimensionally interconnected structure for lithium–sulfur batteries, *J. Power Sources*, 2015, **295**, 182.

11 Y. Qiu, W. Li, W. Zhao, G. Li, Y. Hou, M. Liu, L. Zhou, F. Ye, H. Li and Z. Wei, High-rate, ultralong cycle-life lithium/sulfur batteries enabled by nitrogen-doped graphene, *Nano Lett.*, 2014, **14**, 4821.

12 H. Wang, Y. Yang, Y. Liang, J. T. Robinson, Y. Li, A. Jackson, Y. Cui and H. Dai, Graphene-wrapped sulfur particles as a rechargeable lithium–sulfur battery cathode material with high capacity and cycling stability, *Nano Lett.*, 2011, **11**, 2644.

13 M. Xiao, M. Huang, S. S. Zeng, D. M. Han, S. J. Wang, L. Y. Sun and Y. Z. Meng, Sulfur@graphene oxide core-shell particles as a rechargeable lithium–sulfur battery cathode material with high cycling stability and capacity, *RSC Adv.*, 2013, **3**, 4914.

14 Z. M. Chen, K. Y. Dong, K. Hasegawa, T. Osawa and S. Noda, Over 99.6 wt%-pure, sub-millimeter-long carbon nanotubes realized by fluidized-bed with careful control of the catalyst and carbon feeds, *Carbon*, 2014, **80**, 339.

15 S. W. Lee, B. M. Gallant, Y. M. Lee, N. Yoshida, Y. K. Dong, Y. K. Yamada, S. Noda, A. Yamada and S. H. Yang, Self-standing positive electrodes of oxidized few-walled carbon nanotubes for light-weight and high-power lithium batteries, *Energy Environ. Sci.*, 2012, **5**, 5437.

16 T. Y. Liu, K. C. Kim, B. Lee, Z. M. Chen, S. Noda, S. S. Jang and S. W. Lee, Self-polymerized dopamine as an organic cathode for Li- and Na-ion batteries, *Energy Environ. Sci.*, 2017, **10**, 205.

17 R. Quintero, Y. K. Dong, K. Hasegawa, Y. K. Yamada, A. Yamada and S. Noda, Carbon nanotube 3D current collectors for lightweight, high performance and low cost supercapacitor electrodes, *RSC Adv.*, 2014, **4**, 8230.

18 R. Quintero, D. Kim, K. Hasegawa, Y. Yamada, A. Yamada and S. Noda, Important factors for effective use of carbon nanotube matrices in electrochemical capacitor hybrid electrodes without binding additives, *RSC Adv.*, 2015, **5**, 16101.

19 Y. Chen, S. T. Lu, X. H. Wu and J. Liu, Flexible Carbon Nanotube-Graphene/Sulfur Composite Film: Free-Standing Cathode for High-Performance Lithium/Sulfur Batteries, *J. Phys. Chem. C*, 2015, **119**, 10288.

20 K. Hasegawa and S. Noda, Lithium ion batteries made of electrodes with 99 wt% active materials and 1 wt% carbon nanotubes without binder or metal foils, *J. Power Sources*, 2016, **321**, 155.

21 Z. Yuan, H. J. Peng, J. Q. Huang, X. Y. Liu, D. W. Wang, X. B. Cheng and Q. Zhang, Electrodes: Hierarchical Free-Standing Carbon-Nanotube Paper Electrodes with Ultrahigh Sulfur-Loading for Lithium–Sulfur Batteries, *Adv. Funct. Mater.*, 2015, **24**, 6244.

22 A. A. Abdelhamid, Y. Yu, J. Yang and J. Y. Ying, Generalized Synthesis of Metal Oxide Nanosheets and Their Application as Li-Ion Battery Anodes, *Adv. Mater.*, 2017, **29**, 1701427.

23 M. S. Whittingham, Lithium Batteries and Cathode Materials, *Chem. Rev.*, 2004, **104**, 4271.

24 J. Rong, M. Ge, X. Fang and C. Zhou, Solution ionic strength engineering as a generic strategy to coat graphene oxide (GO) on various functional particles and its application in high-performance lithium–sulfur (Li–S) batteries, *Nano Lett.*, 2014, **14**, 473.

25 S. W. Lee, B. S. Kim, S. Chen, S. H. Yang and P. T. Hammond, Layer-by-Layer Assembly of All Carbon Nanotube Ultrathin Films for Electrochemical Applications, *J. Am. Chem. Soc.*, 2009, **131**, 671.

26 E. Pollak, N. Levy, L. Eliad, G. Salite, A. Soffer and D. Aurbach, Review on Engineering and Characterization of Activated Carbon Electrodes for Electrochemical Double Layer Capacitors and Separation Processes, *Isr. J. Chem.*, 2008, **48**, 287.

27 A. Hiroki, K. Thomas, C. Franco, R. S. William, S. P. S. Milo, H. W. Alan and R. H. Friend, Work Functions and Surface Functional Groups of Multiwall Carbon Nanotubes, *J. Phys. Chem. B*, 2015, **103**, 8116.

28 P. Stathi, D. Gournis, Y. Deligiannakis and P. Rudolf, Stabilization of Phenolic Radicals on Graphene Oxide: An XPS and EPR Study, *Langmuir*, 2015, **31**, 10508.

29 L. Sun, M. Y. Li, Y. Jiang, W. B. Kong, K. L. Jiang, J. P. Wang and S. S. Fan, Sulfur nanocrystals confined in carbon nanotube network as a binder-free electrode for high performance lithium sulfur batteries, *Nano Lett.*, 2014, **14**, 4044.

30 L. Xiao, Y. Cao, J. Xiao, B. Schwenzer, M. H. Engelhard, L. V. Saraf, Z. Nie, G. J. Exarhos and J. Liu, A soft approach to encapsulate sulfur: polyaniline nanotubes for lithium–sulfur batteries with long cycle life, *Adv. Mater.*, 2012, **24**, 1176.

31 G. M. Zhou, Flexible Nanostructured Sulfur–Carbon Nanotube Cathode with High-Rate Performance for Li–S Batteries, *Energy Environ. Sci.*, 2012, **5**, 8901.

